

High-Energy Neutrinos from Photomeson Processes in Blazars

Armen Atoyan¹ and Charles D. Dermer²

¹*CRM, Universite de Montreal, Montreal H3C 3J7, Canada*

²*Code 7653, Naval Research Laboratory, Washington, DC 20375-5352*

(Dated: October 24, 2018)

Abstract

An important radiation field for photomeson neutrino production in blazars is shown to be the radiation field external to the jet. Assuming that protons are accelerated with the same power as electrons and injected with a -2 number spectrum, we predict that km^2 neutrino telescopes will detect $\gtrsim 1$ neutrinos per year from flat spectrum radio quasars (FSRQs) such as 3C 279. The escaping high-energy neutron and photon beams transport inner jet energy far from the black-hole engine, and could power synchrotron X-ray jets and FR II hot spots and lobes.

PACS numbers: 14.60.Lm, 95.85.Ry, 98.54.Cm, 98.62.Nx, 98.70.Rz

EGRET observations of ≈ 100 MeV - 5 GeV emission from over 60 FSRQs and BL Lac objects established that blazars are, with gamma-ray bursts, among the most powerful accelerators of relativistic particles in nature [1]. The standard blazar model consists of a supermassive black hole ejecting twin jets of relativistic plasma, one of which is pointed towards us. Observations of bright, highly variable nonthermal radiation from blazars mean that regions of intense photon and nonthermal particle energy densities, both of which are needed for efficient photopion production [2, 3], are found in these sources. Blazars therefore represent a potential source of energetic π^\pm -decay neutrinos to be detected by operating and planned high-energy neutrino telescopes [4]. Previous treatments have considered internal synchrotron photons and the direct disk radiation field [5] as targets for high-energy proton interactions in jets, and neutrino production in the cores of AGN (active galactic nuclei) [6]. Here we show that photons from external quasi-isotropic radiation fields, which have earlier been proposed as target photons to be Compton-scattered by nonthermal electrons to γ -ray energies [7], also provide the most important photon source for photomeson production of $\gtrsim 30$ TeV neutrinos in FSRQs. The inclusion of this effect increases neutrino detection rates by more than an order-of-magnitude. Moreover, the neutrinos are formed at energies $\gtrsim 3 \times 10^{13}$ eV rather than at $\gtrsim 10^{17}$ eV [8], which improves prospects for detection.

Strong optical emission lines [9] from the illumination of broad-line region (BLR) clouds reveal bright accretion-disk and scattered disk radiation [7] in the inner regions of FSRQs. BL Lac objects have weak emission lines, so the dominant soft photon source is thought to be the internal synchrotron emission in BL Lac objects. In our analysis of photomeson production in FSRQs, we assume that the quasi-isotropic scattered external radiation field dominates the direct accretion-disk field. The photomeson neutrino spectrum can be calculated once the mean magnetic field and comoving spectral energy density are determined. The measured variability time scale t_{var} and synchrotron (L_s) and Compton (L_C) luminosities determined from the spectral energy distribution of the bright, well-studied blazar 3C 279 [10] implies physical parameters of its jet emission region. Its redshift $z = 0.538$, which implies a luminosity distance $d_L \cong 1.05 \times 10^{28}$ cm for an $\Omega_m = 0.3$, $\Omega_\Lambda = 0.7$ cosmology with a Hubble constant of $65 \text{ km s}^{-1} \text{ Mpc}^{-1}$. A crucial unknown is the Doppler factor $\delta = [\Gamma(1 - \beta_\Gamma \cos \theta)]^{-1}$, where Γ is the bulk Lorentz factor of the relativistic plasma blob, and θ is the angle between the jet and observer directions.

The comoving synchrotron photon energy density is given by $u'_s \cong L_s / (2\pi r_b^2 c \delta^4)$, where

r_b is the comoving radius of the blob, here assumed spherical, and primes denote comoving quantities. The spectral energy density $u_s(\epsilon') \equiv m_e c^2 \epsilon' n'_s(\epsilon')$ (units of ergs s⁻¹ ϵ'^{-1}) of photons with dimensionless comoving energy $\epsilon' = h\nu'/m_e c^2$ is found through

$$\epsilon' u'_s(\epsilon') \cong \frac{2d_L^2 f_s(\epsilon)}{r_b^2 c \delta^4} \cong \frac{2d_L^2 (1+z)^2 f_s(\epsilon)}{c^3 t_{var}^2 \delta^6}, \quad (1)$$

in terms of the νF_ν flux $f_s(\epsilon)$ of the synchrotron component. Here $\epsilon = \delta\epsilon'/(1+z)$, and we relate t_{var} and r_b through the expression $r_b \cong ct_{var}\delta/(1+z)$.

For calculations of $n'_s(\epsilon')$ from 3C 279, we approximate the flux density $F(\epsilon) \propto \epsilon^{-\alpha}$ observed during the flare of 1996 [11] in the form of a continuous broken power-law function, with indices $\alpha_1 \cong 0.5$, $\alpha_2 \cong 1.45$, and $\alpha_3 \cong 0.6$ at frequencies $\nu_0 < \nu \leq \nu_1 = \nu_{pk}$, with $\nu_{pk} \cong 10^{13} \nu_{13}$ Hz, $\nu_1 \leq \nu \leq \nu_2 = 10^{16}$ Hz, and $\nu \geq \nu_2$, respectively. The νF_ν synchrotron radiation flux $f_s(\epsilon)$ reaches a maximum value $f_s(\epsilon_{pk}) \cong 1.7 \times 10^{-10}$ erg cm⁻² s⁻¹ at $\nu = \nu_{pk}$ or $\epsilon = \epsilon_{pk}$. The flaring and three-week average flux of the Compton γ -ray component peaks at ~ 500 MeV and is ~ 20 and ~ 5 -10 times larger than $f_s(\epsilon_{pk})$ at the corresponding times [11]. Using $t_{var}(d) \approx 1$ (in days) for 3C 279 as observed by EGRET [11] during the three week average, one finds from equation (1) with $\delta_{10} \equiv \delta/10$ that

$$u'_s \simeq \epsilon'_{pk} u'_s(\epsilon'_{pk}) \simeq 0.4 [t_{var}(d)]^{-2} \delta_{10}^{-6} \text{ erg cm}^{-3}. \quad (2)$$

If the γ -rays from FSRQs are due to Compton-scattered radiation from external photon fields, then $L_{EC}/L_s \cong u'_{ext}/u_B$ [7], where $L_{EC} = L_C - L_{SSC}$ is the measured power from Compton-scattered external photon fields, and L_{SSC} is the synchrotron-self-Compton (SSC) power. Consequently $u'_{ext} \cong u_B(L_{EC}/L_s) = a u'_s = a L_s / (2\pi r_b^2 c \delta^4)$, where $a \equiv L_{EC}/L_{SSC}$. The energy of the external photons in the comoving frame is $\epsilon'_{ext} \cong \delta \epsilon_{ext}$. Models taking into account SSC and external Compton (EC) components show that a complete spectral fit requires synchrotron, SSC and EC components [12], with $a \sim 0.1$ -1 for BL Lac objects and $a \sim 1$ -10 for FSRQs. During the 1996 flare of 3C 279, $a \simeq 10$, so that the energy density of external soft photons in the comoving blob frame is $\sim 10\times$ greater than the synchrotron energy density. Moreover, the energy of these photons increases with δ , lowering the photomeson production threshold.

Lower limits to δ are defined by the condition that the emitting region be transparent to $\gamma\gamma$ pair-production attenuation inside the blob [13], which requires that $\tau_{\gamma\gamma}(\epsilon') \cong 2\sigma_T n'_s(2/\epsilon') r_b / (3\epsilon') < 1$. The measured $> 10^{16}$ Hz flux during the 1996 flare then implies that $\delta \geq 5[E_{ph}(\text{GeV})^{0.12} / t_{var}(d)^{0.19}]$, where $E_{ph}(\text{GeV})$ is the photon energy in GeV.

The magnetic field B in the blob can be determined by introducing the equipartition parameter $\eta = u'_{el}(1 + k_{pe})/u_B$ for the ratio of relativistic electron to magnetic energy densities in the jet, with the factor k_{pe} correcting for the presence of nonthermal hadrons. We assume $k_{pe} = 1$ in the estimate of B . The measured synchrotron flux density $F_s \propto \epsilon^{-\alpha}$ with $\alpha \simeq 0.5$ at $\nu \lesssim 10^{13}$ Hz gives the equipartition magnetic field

$$B(\text{Gauss}) \cong 130 \frac{d_{28}^{4/7} f_{-10}^{2/7} [(1 + k_{pe}) \ln(\nu_0/\nu_1)]^{2/7} (1+z)^{5/7}}{\eta^{2/7} [t_{\text{var}}(\text{d})]^{6/7} \delta^{13/7} \nu_{13}^{1/7}} \quad (3)$$

where $\nu_0/\nu_1 \cong 10^3$ and $f_{-10} \equiv f_s(\epsilon_{pk})/(10^{-10} \text{ erg cm}^{-2} \text{ s}^{-1}) = 1.7$ for 3C 279.

An alternative estimate of B can be derived from the observed synchrotron and Compton powers [14]. Neglecting Klein-Nishina effects on Compton scattering, the ratio of the Compton and synchrotron powers $L_C/L_s \cong u'_{ph}/u_B$, so that $u_B = (L_s/L_C)u'_s(1 + u'_{ext}/u'_s) = (L_s/L_C)u'_s(1 + a)$. Using equation (1) in this expression for B gives

$$B(\text{Gauss}) \cong \frac{2(1+z)}{\delta^3 t_{\text{var}}} \frac{L_s \sqrt{1+a}}{c^{3/2} L_C^{1/2}}. \quad (4)$$

The observed flux of synchrotron radiation from 3C 279 with $\alpha = 0.5$ at $\nu \ll 10^{13}$ Hz implies that $B(\text{G}) \simeq 7 \eta^{-2/7} [t_{\text{var}}(\text{d})]^{-6/7} \delta_{10}^{-13/7}$ from equipartition arguments. The estimate of B from equation (4) gives $B(\text{G}) \cong 4 t_{\text{var}}^{-1}(\text{d}) \delta_{10}^{-3}$, using $L_s = 3 \times 10^{47} \text{ ergs s}^{-1}$, $L_C/L_s \cong 10$, and $a \cong 10$. The external radiation energy density in the comoving frame, using B derived from equation (3), is $u'_{ext} \simeq 1.5 (L_{EC}/L_s) \eta^{-4/7} [t_{\text{var}}(\text{d})]^{-12/7} \delta_{10}^{-26/7} \text{ erg cm}^{-3}$. Note the weaker dependence of u'_{ext} on δ compared to u'_s . For the calculations we take $\eta = 1$ and $L_{EC}/L_s = 10$.

Energy losses of relativistic protons (and neutrons) are calculated on the basis of standard expressions (e.g., Ref. [15]) for the cooling time of relativistic protons due to photopion production in $p\gamma$ collisions. If the ambient photons have spectral density $n'_{\text{ph}}(\epsilon')$, then

$$t_{p\gamma}^{-1}(\gamma_p) = \int_{\frac{\epsilon_{\text{th}}}{2\gamma_p}}^{\infty} d\epsilon' \frac{c n'_{\text{ph}}(\epsilon')}{2\gamma_p^2 \epsilon'^2} \int_{\epsilon_{\text{th}}}^{2\epsilon'\gamma_p} d\epsilon_r \sigma(\epsilon_r) K_{p\gamma}(\epsilon_r) \epsilon_r,$$

where γ_p is the proton Lorentz factor, ϵ_r is the photon energy in the proton rest frame, $\sigma(\epsilon_r)$ is the photopion production cross section, $\epsilon_{\text{th}} \approx 150 \text{ MeV}$ is the threshold energy for the parent photon in the proton rest frame, and $K_{p\gamma}(\epsilon_r)$ is the inelasticity of the interaction. The latter increases from $K_1 \approx 0.2$ at energies not very far above the threshold, to $K_2 \sim 0.5 - 0.6$ at larger values of ϵ_r where multi-pion production dominates [15, 16].

A detailed recent study of this photohadronic process is given by Ref. [16]. To simplify calculations, we approximate $\sigma(\epsilon_r)$ as a sum of 2 step-functions $\sigma_1(\epsilon_r)$ and $\sigma_2(\epsilon_r)$ for the total

single-pion ($p+\gamma \rightarrow p+\pi^0$ or $n+\pi^+$) and multi-pion channels, respectively, with $\sigma_1 = 380 \mu\text{b}$ for $200 \text{ MeV} \leq \epsilon_r \leq 500 \text{ MeV}$ and $\sigma_1 = 0$ outside this region, whereas $\sigma_2 = 120 \mu\text{b}$ at $\epsilon_r \geq 500 \text{ MeV}$. The inelasticity is approximated as $K_{p\gamma} = K_1$ and $K_{p\gamma} = K_2$ below and above 500 MeV. Our calculations give good agreement with more detailed treatments of the time scales for photopion interactions of ultra-relativistic cosmic rays with the cosmic microwave background [15, 17]. This approach also works well for a broad power-law distribution of field photons $u'_{\text{ph}}(\epsilon') \propto (\epsilon')^{-\alpha}$ for different spectral indices α , and readily explains the significant increase in the mean inelasticity of incident protons (or neutrons) from $\langle K_{p\gamma} \rangle \simeq 0.2$ for steep photon spectra with $\alpha_\gamma \gtrsim 1$, to $\langle K_{p\gamma} \rangle \rightarrow 0.6$ for hard spectra with $\alpha_\gamma < 1$ [16].

The spectra of secondary $\pi^{0,\pm}$ -decay particles (ν , γ , e) are calculated in the δ -function approximation, assuming that the probabilities for producing pions of different charges (π^0 , π^+ and π^-) are equal for the multi-pion interaction channel. To correctly apply the δ -function approximation, one has to properly take into account the different inelasticities of the multi-pion and single-pion production channels (see Ref. [16] for comparison).

We assume that the spectrum of the external UV radiation field arises from a Shakura/Sunyaev [18] optically-thick accretion disk model that is scattered by BLR clouds, though other sources of external photons could be reprocessed line emission or infrared radiation from a torus. This disk model has flux density $F(\epsilon) \propto \epsilon^{1/3} \exp(-\epsilon/\epsilon_{max})$, where the maximum photon energy ϵ_{max} is determined by the innermost radius of the blackbody disk and properties of the central engine. We take $m_e c^2 \epsilon_{max} = 35 \text{ eV}$ [19].

Fig. 1 shows observer-frame energy loss timescales of protons due to photopion production in a jet of 3C 279 calculated for Doppler-factors $\delta = 7, 10$, and 15. For comparison, we show also the photopion timescales if only the interactions with the synchrotron radiation were taken into account for the cases $\delta = 7$ and 10. Fig. 2 shows the energy distributions of relativistic protons $N_p(E)$ in the jet plasma blobs calculated assuming power-law injection of relativistic protons with number index $\alpha_p = 2$ on observed timescales $\Delta t = 3$ weeks. The total injection power of the protons $L_p = 2 \times 10^{48} \delta^{-4} \text{ erg s}^{-1}$, which corresponds to the average measured γ -ray luminosity from 3C 379 during the three week observing period surrounding the 1996 flare [11]. In calculations of N_p we take into account the photohadron interaction energy losses, as well as the escape losses of the protons in the Bohm diffusion limit. This limit ensures that the gyroradii $r_L(\text{cm}) \cong 3.1 \times 10^6 (A\gamma_p/Z)/B(\text{G})$ of the highest energy ions do not exceed r_b [20].

Importantly, we also take into account proton losses through the $p\gamma \rightarrow nX$ channel. The neutrons may then escape the blob either before they decay or collide again with photons inside the blob. To demonstrate the significance of this channel, in Fig. 2 by the full dotted curve we show the proton distribution calculated for the case of $\delta = 7$, but neglecting the effect of escaping neutrons. Comparison with the solid curve indicates that $\simeq 50\%$ of the $E \geq 10^{14}$ eV proton energy is carried by relativistic neutrons from the blob, forming a highly collimated neutron beam with opening angle $\theta_b \sim 1/\Gamma$ and a total power $L_n^{(beam)} \sim 0.25L_p \sim 5 \times 10^{47}\delta^{-4}$ erg s $^{-1}$ for the parameters assumed in Fig. 2.

Fig. 3 shows the expected differential fluences of neutrinos produced by protons in Fig. 2, integrated over the 3 week flaring period. Note that the mean neutrino energy fluxes at $E \geq 100$ TeV are at the level $E F_\nu(E) \simeq E^2 \Phi_\nu / \Delta t \lesssim 2 \times 10^{-11}$ erg cm $^{-2}$ s $^{-1}$. Given very similar emissivities in overall secondary ν and $(\gamma + e)$ production (e.g. Ref. [16]), the *unabsorbed* fluxes of multi-TeV γ -rays would therefore be at the same level, which makes only $\leq 2\%$ of the γ -ray energy flux detected by EGRET. A pair-photon cascade in the blob would increase this fraction to the level of $\leq 10\%$ contribution of the cascade radiation to the detected γ -ray flux, reprocessing most of the initial γ -ray energy into γ -radiation with $E \lesssim 10$ GeV. A small fraction of the energy will appear as synchrotron radiation in the X-ray to GeV γ -ray band. Because the cascade synchrotron power is emitted with a very hard spectrum over a wide energy range, it will not overproduce also the observed X-ray flux of 3C 279. These estimates show, however, that the nonthermal proton power cannot be more than $10\times$ the γ -ray power, or the cascade radiation would exceed the observed fluxes.

For the fluences in Fig.4, the total number N_ν of neutrinos that could be detected by a 1 km 2 detector, using neutrino detection efficiencies given by Ref. [4], is 0.45, 0.27 and 0.12 for the cases of $\delta = 7, 10$ and 15, respectively. These numbers are, however, much less if the external field is neglected, giving instead the values $N_\nu \approx 0.055$ ($\delta = 7$) and 0.014 ($\delta = 10$) for the fluences in Fig. 3. This would not leave a realistic prospect for the detection of at least 2-3 neutrinos, which is required for a positive detection of a source. BL Lac objects, which have weak BLRs and, therefore, a weak scattered external radiation field, should consequently be much weaker neutrino sources.

For a 10% flaring duty factor, and considering the additional neutrino production during the quiescent phase, we expect that IceCube or other km 2 array may detect several neutrinos per year from 3C 279-type blazar jets with $\delta \approx 5$ -15. Allowing an overall power of protons

larger than that for primary electrons improves the prospects for neutrino detection. A softer nonthermal proton spectrum would, however, reduce the neutrino emissivity.

Acceleration of protons only to $E_p \gtrsim 10^{14}$ eV is required for efficient neutrino production through photomeson interactions, as can be seen from Fig.1. Thus we predict that a km² array will detect high-energy neutrinos from FSRQs without requiring acceleration of protons to ultra-high ($\gtrsim 10^{19}$ eV) energies. The maximum cosmic-ray energies from blazars are found to be $E_{CR,max} \simeq 8 \times 10^{17} Z \Gamma^2 B(G) t_{var}(d)/(1+z)$ eV [20], with maximum neutrino energies a factor ~ 20 lower. Given additionally the intense photomeson interactions encountered by a proton at this optimistic limit in the jet environment (see Fig. 1), it is unlikely that the inner jets of blazars are significant sources of ultra-high energy cosmic rays. The neutrino production from FSRQs is therefore unaffected by the cosmic ray bound of Ref. [21] (though note the more general upper limit derived in Ref. [3]).

About half of the photomeson interactions in the plasma jet will produce neutrons. Neutrons with comoving Lorentz factors $\gamma'_n \gtrsim 10^3 \delta_{10} t_{var}(d)$ will escape the blob in a collimated beam, and continue to interact efficiently with the external UV radiation field up to $\sim 0.1-1$ pc scales, initiating pair-photon cascades far away from, but in the same direction with, the inner jet due to secondary γ -rays and electrons. FSRQ jets will thus form intense neutron and photon beams that transport energy far from the central engine of the AGN [22]. Cosmic-ray neutrons with energies of $10^{17} E_{17}$ eV will decay at distances $\lesssim E_{17}$ kpc from the jet core. The deposition of the energy of the beamed hadrons and multi-TeV γ -rays (through $\gamma\gamma$ -absorption at > 10 kpc scales) can reasonably be at the mean rate $\sim 10^{43}$ erg s⁻¹, which could lead to enhanced X-ray synchrotron emission along the large-scale jet, as seen by the *Chandra X-ray Observatory* from sources such as Pictor A [23]. Depending on the stability of charged particle transport, nonthermal particles could be deposited at $\gtrsim 100$ kpc to supply power for hot spots and lobes in FR II galaxies, though *in situ* particle acceleration could also take place at these sites. The predicted weaker neutron and neutrino production in BL Lac objects and their parent FR I galaxies might account for the morphological differences of these radio galaxy types. This picture will be tested by sensitive high-energy neutrino detectors, ground-based $\gtrsim 50$ GeV gamma-ray detectors, and *GLAST* [4, 24].

AA appreciates the support and hospitality of the NRL Gamma and Cosmic Ray Astrophysics Branch during his visit when this work was initiated. The work of CD is supported

by the Office of Naval Research and NASA grant DPR S-13756G.

- [1] R.C. Hartman *et al.*, *Astrophys. J. Suppl.* **123**, 79 (1999).
- [2] K. Mannheim and P.L. Biermann, *Astron. Astrophys.* **253**, L21 (1992).
- [3] K. Mannheim, R.J. Protheroe, and J.P. Rachen, *Phys. Rev. D* **63**, 023003 (2001).
- [4] T.K. Gaisser, F. Halzen, and T. Stanev, *Phys. Repts.*, **258(3)** 173 (1995); F. Halzen, in *High Energy Gamma Ray Astronomy*, ed. F.A. Aharonian and H.J. Völk (AIP: New York), p. 43 (2001).
- [5] K. Mannheim, T. Stanev, and P.L. Biermann, *Astron. Astrophys.* **260**, L1 (1992); K. Mannheim, *Astron. Astrophys.* **269**, 67 (1993); W. Bednarek and R.J. Protheroe, *MNRAS*, **302**, 373 (1999).
- [6] F.W. Stecker *et al.*, *Phys. Rev. Lett.* **66**, 2697 (1991), F.W. Stecker *et al.*, *Phys. Rev. Lett.* **69**, 2738 (1992).
- [7] M. Sikora, M.C. Begelman, and M.J. Rees, *Astrophys. J.* **421**, 153 (1994); C.D. Dermer, S.J. Sturmer, and R. Schlickeiser, *Astrophys. J. Suppl.* **109**, 103 (1997).
- [8] A. Mücke and R.J. Protheroe, in *Proc. 27th International Cosmic Ray Conference, Hamburg, Germany (astro-ph/0105543)* (2001).
- [9] H. Netzer, in *Active Galactic Nuclei*, ed. T. J.-L. Courvoisier and M. Mayor (New York: Springer), p.57.
- [10] R.C. Hartman *et al.*, *Astrophys. J.* **461**, 698; E. Pian *et al.*, *Astrophys. J.* **521**, 112 (1999).
- [11] A.E. Wehrle *et al.*, *Astrophys. J.* **497**, 178 (1998)
- [12] M. Böttcher, *Astrophys. J.* **515**, L21 (1999); R.C. Hartman *et al.*, *Astrophys. J.* **553**, 683 (2001); R. Mukherjee *et al.*, *Astrophys. J.* **527**, 132 (1999).
- [13] L. Maraschi, G. Ghisellini, and A. Celotti, *Astrophys. J.* **397**, L5 (1992); C.D. Dermer and N. Gehrels, *Astrophys. J.* **447**, 103, (e) *Astrophys. J.* **456**, 412 (1996).
- [14] Tavecchio, F., Maraschi, L., & Ghisellini, G. , *Astrophys. J.* **509**, 608 (1998).
- [15] V. S. Berezhinskii and S. I. Grigoreva, *Astron. Astrophys.* **199**, 1 (1988).
- [16] A. Mücke, J.P. Rachen, R. Engel, R.J. Protheroe, and T. Stanev, *Pub. Astron. Soc. Australia* **16**, 160 (1999).
- [17] T. Stanev, R. Engel, A. Mücke, R.J. Protheroe, and J.P. Rachen, *Phys. Rev. D* **62**, 093005

- (2000).
- [18] N.I. Shakura and R.A. Sunyaev, *Astron. Astrophys.* **24**, 337 (1973).
 - [19] C.D. Dermer and R. Schlickeiser, *Astrophys. J.* **416**, 458 (1993).
 - [20] A.M. Hillas, *Ann. Rev. Astron. Astrophys.* **22**, 425 (1984); C.A. Norman, D.B. Melrose, and A. Achterberg, *Astrophys. J.* **454**, 60 (1995).
 - [21] See E. Waxman and J. Bahcall, *Phys. Rev. D* **59**, 023002 (1998); J. Bahcall and E. Waxman, hep-ph/9902383. Limitations of this bound are discussed by R.J. Protheroe, astro-ph/9809144.
 - [22] A.M. Atoyan, *Astron. Astrophys.* **257**, 465 (1992); A.M. Atoyan, *Astron. Astrophys.* **257**, 476 (1992).
 - [23] A.S. Wilson, A.J. Young, and P.L. Shopbell, *Astrophys. J.* **547**, 740 (2001).
 - [24] For information about the *Gamma ray Large Area Space Telescope*, see glast.gsfc.nasa.gov.

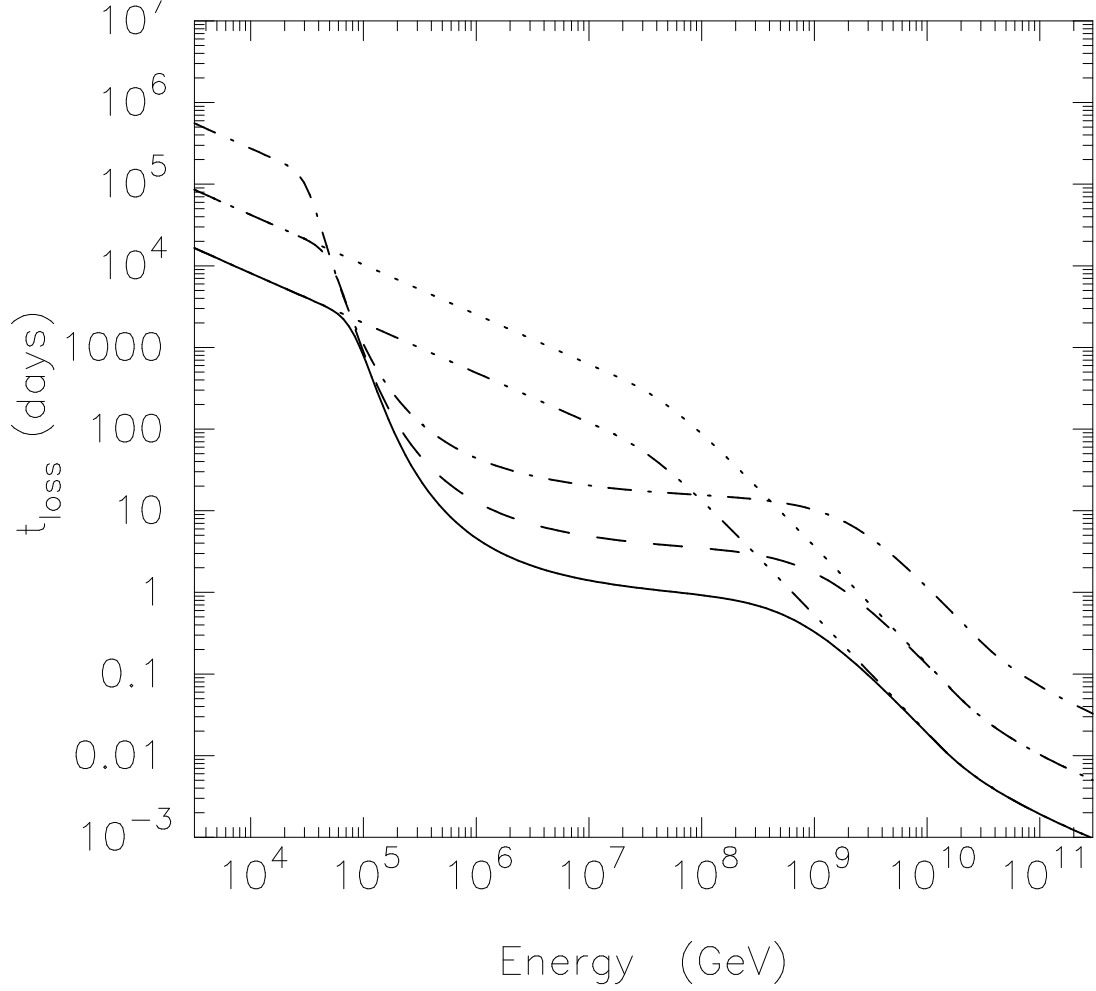


FIG. 1: Photomeson interaction energy loss time scale of protons, calculated for spectral fluxes observed from 3C 279 (see text) and $t_{\text{var}} = 1$ d, assuming 3 different Doppler-factors for the jet: $\delta = 7$ (solid curve), $\delta = 10$ (dashed curve), and $\delta = 15$ (dot-dashed curve). The dotted and triple-dot-dashed curves are calculated for $\delta = 7$ and $\delta = 10$, respectively, when $p\gamma$ interactions with the synchrotron radiation field alone are considered.

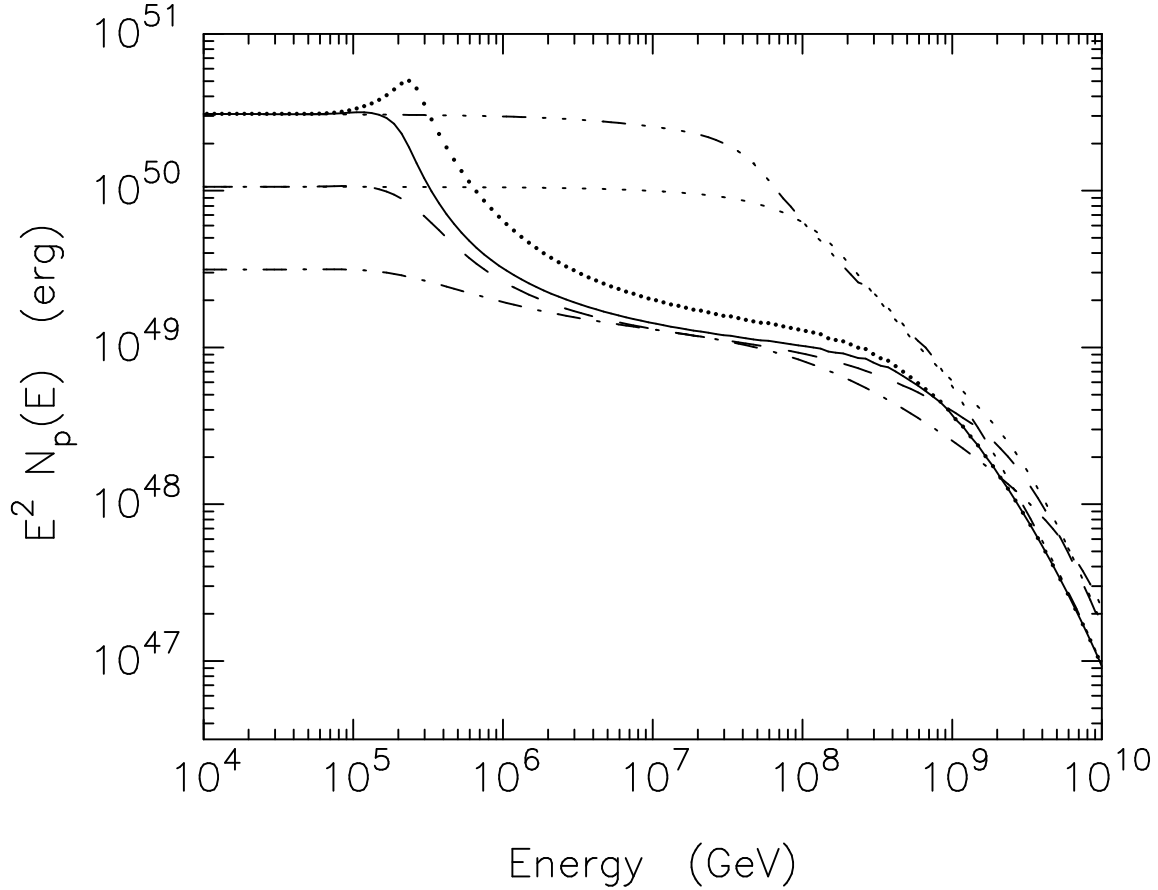


FIG. 2: The energy distribution of relativistic protons, calculated for the same jet Lorentz-factors $\delta = 7, 10,$ and 15 and assumptions for the external and internal radiation fields as made in Fig. 1, assuming a power-law injection of relativistic protons with number index $\alpha_p = 2$ during $\Delta t = 3$ weeks with a power $L_p = 2 \times 10^{48} \delta^{-4}$ ergs s^{-1} . The full dots show the proton distribution calculated without the effect of neutrons escaping the blob.

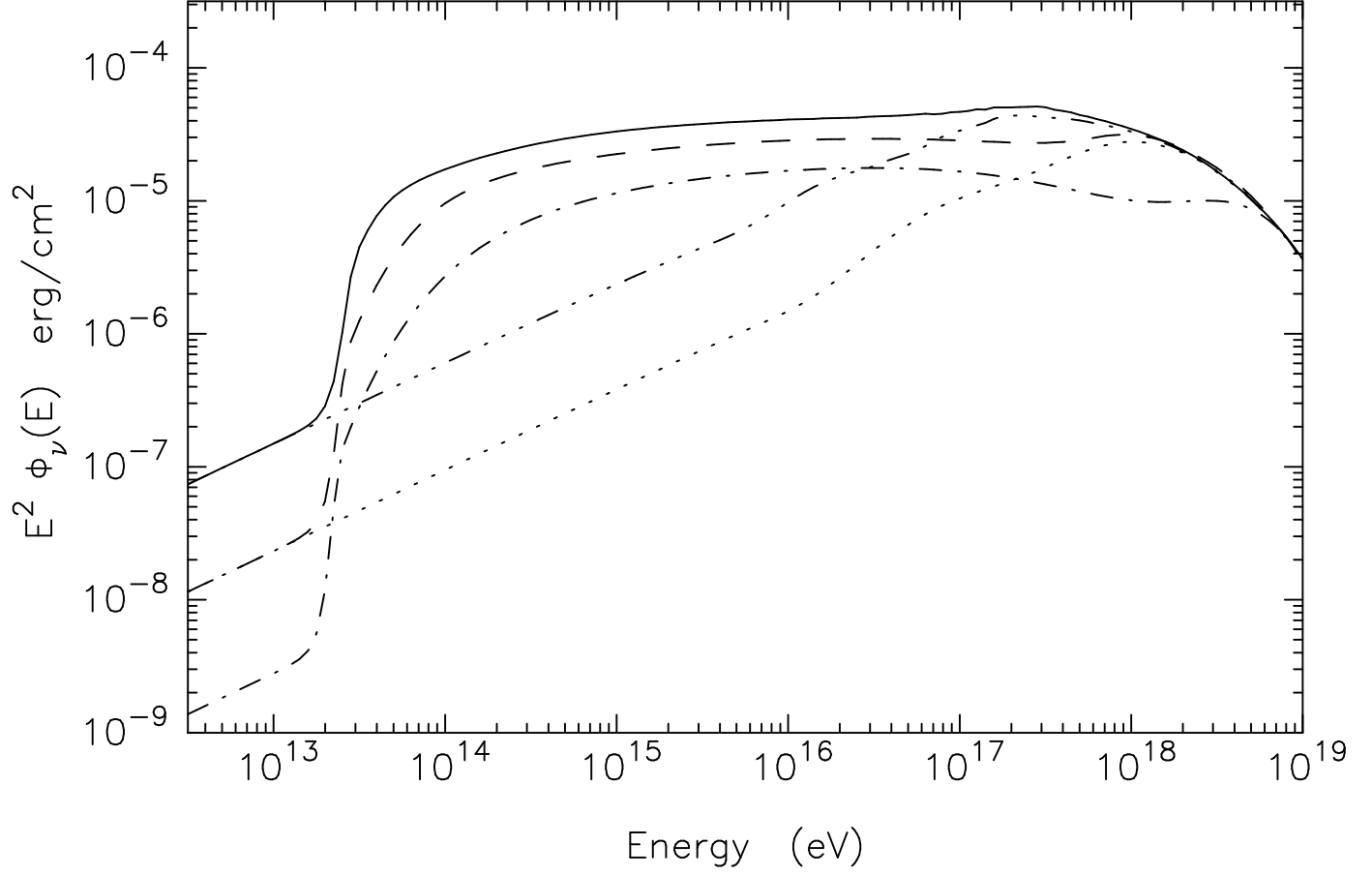


FIG. 3: The fluences of neutrinos expected due to photomeson interactions of protons shown in Fig. 2 with the external (UV) and internal (synchrotron) photons in the jet of 3C 279 for Doppler factors $\delta = 7$ (solid curve) $\delta = 10$ (dashed curve), and $\delta = 15$ (dot-dashed curve). The dotted and triple-dot-dashed curves show the neutrino fluences if the external photon field in the jet is neglected.